Document Type	Analysis Report
Document Number	ESS-0136227
Date	Aug 18, 2020
Revision	10
State	Released
Confidentiality Level	Internal
Page	1 (18)

Source terms for the ESS normal conducting linac beam commissioning

	Name	Role/Title
Owner	Douglas Di Julio	Radiation Physicist
Reviewer	Riccardo Bevilacqua	Radiation Protection Expert
Approver	Mamad Eshraqi Günter Muhrer Sigrid Kozielski	Accelerator Physicist ESS Shield Design Coordinator Group Leader Radiation Protection
Distribution list	Mats Lindroos John Weisend	Head of Accelerator Division Deputy Head of Accelerator Project

TABLE OF CONTENT **PAGE**

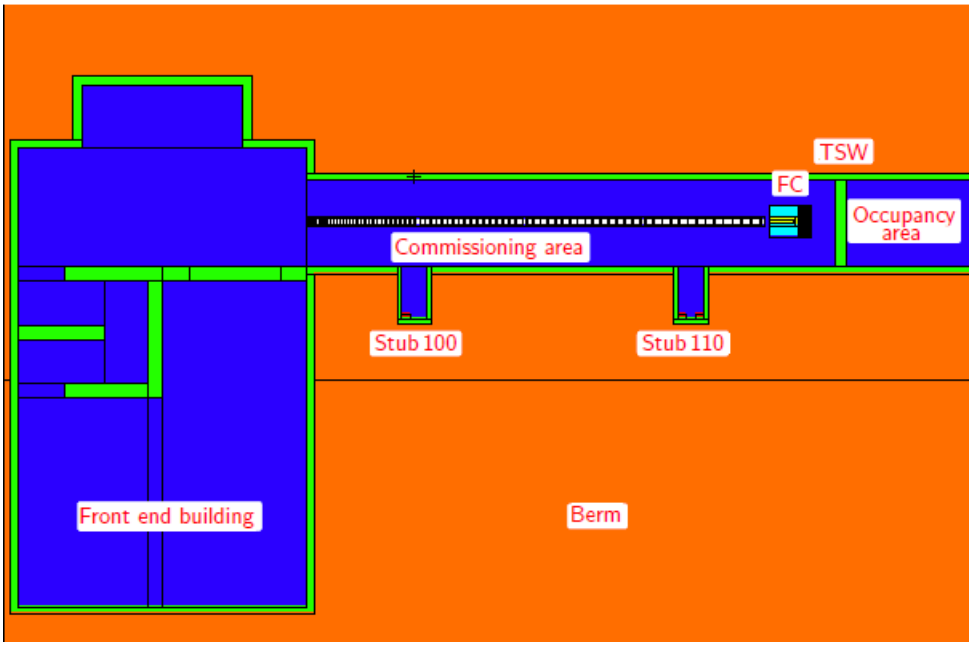

Figure 1: Horizontal cut through the normal conducting linac tunnel with 4 DTL tanks installed.

1. SCOPE

Shielding calculations for the ESS proton linear accelerator (linac) are presented in [1]. The shielding is being built and a majority of it is the concrete structure of the linac tunnel and a soil (berm) around it.

However, during the early stages of operation, a normal conducting linac (up to DTL tank 4) commissioning is planned in the first part of the tunnel, while installation of the superconducting linac components is on-going in the downstream part of the tunnel[1].

The scope of this document is to calculate the prompt dose rates behind the temporary shielding wall (TSW). The dose rate requirements are defined in [2] for supervised and non-designated areas. Specifically, prompt-dose rate values up to the location of a fence placed behind the TSW are calculated and also the position of a second fence, placed further downstream for the 74 MeV case, described below, is determined. Calculations to determine the dose rate behind the TSW due to an increase in beam energy of 76 MeV were also carried out.

A Faraday cup [3] was chosen as a temporary beam stop for beam energies up to the end of DTL tank 4, of approximately 74 MeV, and for the commissioning stage. The Faraday cup (FC) is surrounded by shielding. Additionally, a temporary shielding wall will separate commissioning and occupancy areas of the linac as shown in Fig. 1.

[1] DTL tank 5 is excluded from initial installation, in order to allow space for FC and shielding, which is required for the normal conducting linac commissioning (up to DTL tank 4), while installing the superconducting linac.

Additionally, the tunnel air activation is reported, in order to serve as input for other calculations outside the scope of this document.

2. CONTRIBUTORS

Input was provided by the beam physics, operations and beam diagnostics group of accelerator division related to a Faraday cup design (geometry and materials) [3] and proton beam parameters [4]. Geometry definition of the opening for the chicane in the TSW and the first fence position was provided by Wolfgang Hees and Mamad Eshraqi.

3. ISSUING ORGANISATION

Spallation Physics Group , Target Division, European Spallation Source

4. METHODOLOGY

A shielding design procedure for safety [5] was followed when designing the shielding. A simplified geometry model of the normal conducting linac was used as a baseline. The Faraday Cup with its shielding as well as temporary shielding wall between commissioning and occupancy areas were added in the model.

For the activation calculations, the door and the chicane/pipe penetrations in the TSW were not modelled. They were taken into account for the beam on FC and 1 W/m calculations when the mechanical design of the penetrations became available.

5. ACCEPTANCE CRITERIA

NA. Acceptance discussions are discussed in the hazard analysis documentation. The 1 W/m losses are to be scaled according to [6].

6. OPEN ITEMS

Results outside of the peak dose-rate regions and in particular for photons and the 1 W/m calculations are limited and can have higher uncertainties.

7. ASSUMPTIONS

Calculations were performed with two source terms described in Sec. 10.2.

8. LIMITATIONS

The geometry model is simplified. Other limitations are related to the items described in the methodology and open items section.

9. COMPUTER HARDWARE AND SOFTWARE

Monte-Carlo calculations performed with MCNP6.2 [7] used the CEM03 model [8,9,10] coupled with the ENDF/B-VII.0-based neutron libraries [11] for the beam on FC4 at 74 MeV calculation. The other two FC cases used DXTRAN spheres combined with the la150 libraries packaged with MCNP and the TENDL-2017 [12] libraries.

The air activation calculations described in Sec. 12 were performed with PHITS 2.23 [13] using the INCL 4.6 [14] and GEM [15] models coupled with the ENDF/B-VII.0-based neutron libraries [11].

The calculations with the 1 W/m source were carried out using PHITS 3.1 [16] with neutron data libraries taken from ENDF/B-VII.1/VIII [17,18] and using the INCL [19] and KUROTAMA models [20].

The geometric models were created using the CombLayer [21] tool, which can create identical geometries in PHITS and MCNP.

When weight windows were used, there were generated using ADVANTG 3.0.3 [22].

10. CALCULATION INPUTS

10.1. Geometry and Materials

Geometry The model geometry views of the normal conducting linac components, FC and TSW are shown in Fig. 1-8, which use centimetres as dimension units.

The FC shielding dimensions used in the activation calculations differ from the FC shielding used in the other sections because this work was carried out before the mechanical design of the FC shielding was completed. Both geometries are compared in Fig. 2 and 3.

The door and air ventilation chicane/penetrations in the TSW were modelled only for the FC calculations and 1 W/m calculations, after the final TSW thickness was defined and the mechanical design of the penetrations was implemented. In the activation calculations, the TSW was modelled as a solid block of SkanskaConcrete. Penetrations which included cable filler material were assumed to be filled at a 50% filling fraction. This was modelled by adjusting the density of the filler material by 50%. The StdTCABL material was used for this and taken from the model described in [1].

The air ventilation chicane is modelled as a uniform opening of 40 cm in height and 30 cm in width. The second leg of the chicane is approximately 1.5 m in length.

Materials The materials used in the simulations are shown in the corresponding figures and described in Table 1-5.

The SkanskaConcrete material definition was borrowed from [1], where the material is defined in the MARS format (see Table 2). This definition was translated into MCNP format shown in Table 3. Note that in the MARS definition the natural isotopic abundance of the elements is assumed, while for MCNP individual isotopes had to be explicitly defined in order to be able to use the ENDF/B-VII.0 neutron libraries [11]. The composition for the mild steel in the TSW was taken from [23].

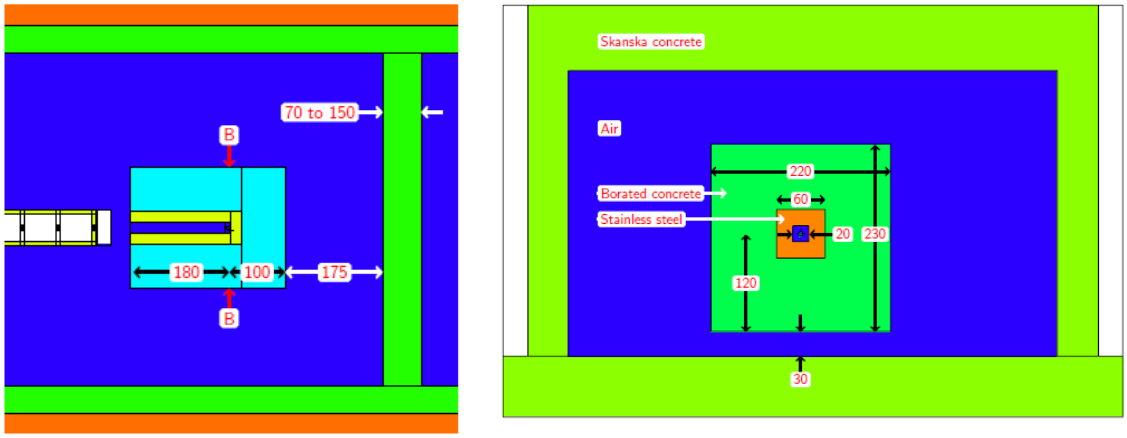

Figure 2: Geometry of the FC with shielding and TSW area as used in the activation section 12. (Left) Horizontal cut and (Right) Section view B-B indicated on the left figure.

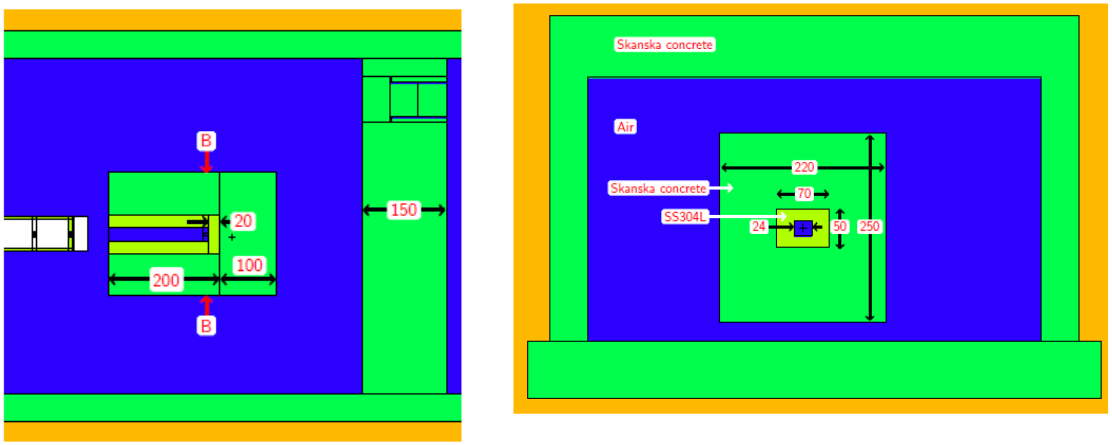

Figure 3: Geometry of the FC with shielding and TSW area as used in section 11. (Left) Horizontal cut and (Right) Section view B-B indicated in the left figure.

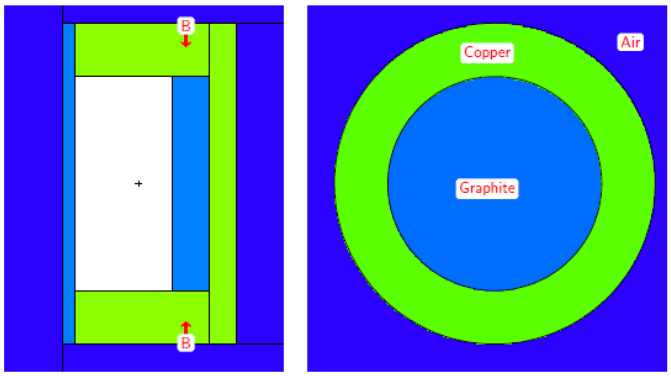

Figure 4: DTL 2 FC views. (Left) Horizontal cut and (Right) Section B-B indicated in the left figure.

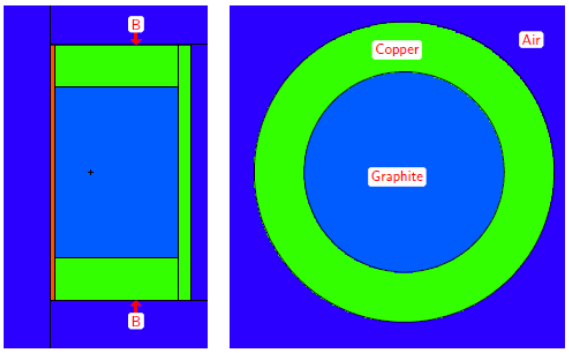

Figure 5: DTL 4 FC views. (Left) Horizontal cut and (Right) Section view B-B indicated in the left figure.

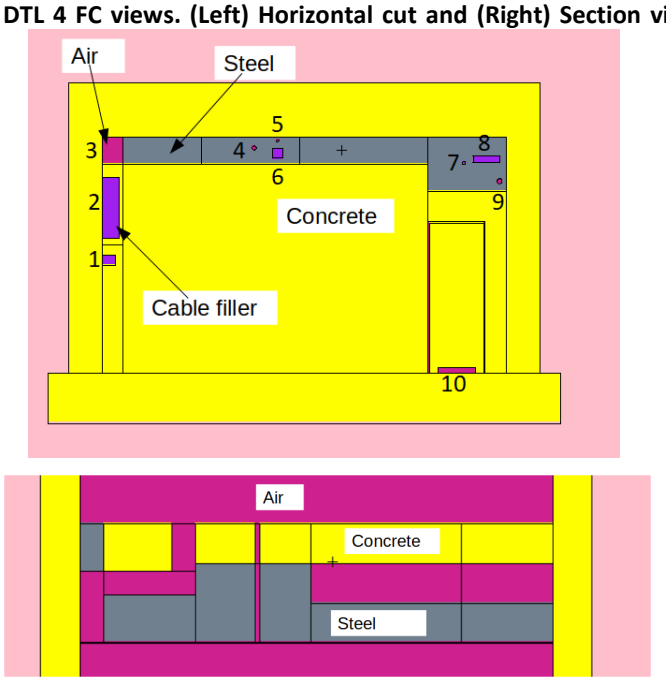

1)	h=15 w=20
2)	h=90 w=25
3)	h=40 w=30
4)	r=3.2
5)	r=2
6)	15 x 15
7)	r=2.5
8)	h=10 w=39
9)	r=4
10)	h=8 w=55

Figure 6: Views of the TSW as used in section 11. (Top) Vertical cut showing the TSW wall side facing the NC accelerator and (Bottom). The upper portion of the wall where the air ventilation chicane is located. The labelled penetration sizes in cm are given in the table on the right.

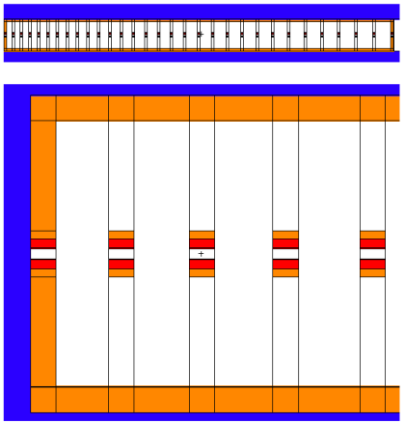

Figure 7: (Top) Horizontal cut through DTL1 and (Bottom) Enlarged view of the first five PMQs.

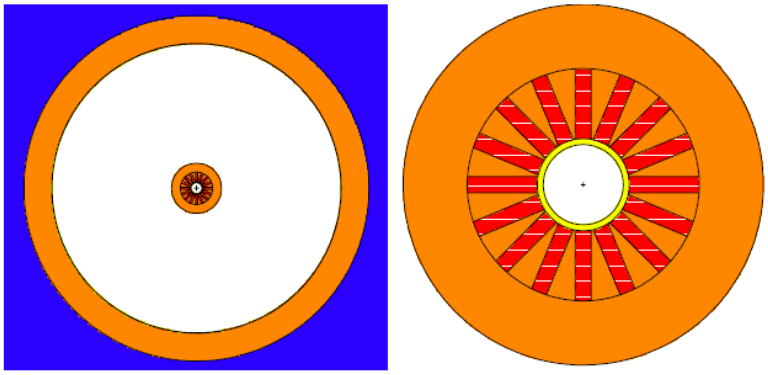

Figure 8: (Left) Vertical cut through a DTL with a PMQ at the center and (Right) an enlarged view of the PMQ.

Table 1: List of Materials

Material	Density [g/cm³]	MCNPX definition		Description
Air	$1.20 \cdot 10^{-3}$	6000.70c 7014.70c 8016.70c 18036.70c 18038.70c 18040.70c	7.0000e-09 3.9128e-05 1.0512e-05 8.1682e-10 1.3987e-10 2.3207e-07	Dry air near sea level
Graphite	1.70	6000.70c 5010.70c 5011.70c	8.523759e-02 1.894100e-08 7.576401e-08	
Skanska concrete	2.35	See Table 3		
Borated concrete	2.31	99 % Skanska concrete and 1 % natural Boron (mass fraction)		
Copper	8.94	29063.70c 29065.70c	0.058389212 0.02604927	Oxygen-free copper. Information about impurities is not available.
Stainless steel	7.85	6000.70c 14028.70c 14029.70c 14030.70c 15031.70c 16032.70c 16033.70c 16034.70c 16036.70c 24050.70c 24052.70c 24053.70c 24054.70c 25055.70c 26054.70c 26056.70c 26057.70c 26058.70c 28058.70c 28060.70c 28061.70c 28062.70c 28064.70c	0.001366050 0.017958587 0.000912310 0.000602105 0.000794573 0.000486055 0.000003838 0.000021747 0.000000051 0.008683351 0.167449786 0.018987462 0.004726381 0.019910026 0.038864395 0.610087892 0.014089590 0.001875066 0.063434555 0.024434877 0.001062167 0.003386654 0.000862481	SS304L as defined in [24]. Information about impurities is not available.
Samarium Cobalt	8.40	27059.70c 62147.70c 62149.70c 62150.70c 62152.70c	8.5 0.521 0.138 0.074 0.267	Sm_2Co_{17}
TZM	10.22	See Table 4		

Table 2: SkanskaConcrete as defined in MARS [1]

A	Z	Mass fraction
1.008	1.0	3.35720233139058521e-03
15.999	8.0	3.82342797668609513e-01
24.305	12.0	0.0019
26.9815385	13.0	0.0192
28.085	14.0	0.1251
32.059	16.0	0.0081
39.0983	19.0	0.0158
40.078	20.0	0.3927
47.867	22.0	0.0038
54.938044	25.0	0.0021
55.845	26.0	0.0444
58.6934	28.0	0.0012

Table 3: SkanskaConcrete definition

Element	Atomic fraction
1001.70c	7.59312534134E-02
1002.70c	8.71640551643E-06
8016.70c	5.43526947592E-01
8017.70c	2.06950892017E-04
8018.03c	1.11647473471E-03
12024.70c	1.40785315301E-03
12025.70c	1.78230050329E-04
12026.70c	1.96234647556E-04
13027.70c	1.62241753736E-02
14028.70c	9.36645875617E-02
14029.70c	4.75605601141E-03
14030.70c	3.13523026267E-03
16032.70c	5.46727493842E-03
16033.70c	4.37717251109E-05
16034.70c	2.47073209942E-04
16036.70c	1.15370377360E-06
19039.70c	8.59239038130E-03
19040.70c	1.07825377081E-06
19041.70c	6.20088236070E-04
20040.70c	2.16565974405E-01
20042.70c	1.44539631664E-03
20043.70c	3.01589179418E-04
20044.70c	4.66011784421E-03
20046.70c	8.93555255277E-06
20048.70c	4.17755887748E-04
22046.70c	1.49322931163E-04
22047.70c	1.34665826718E-04
22048.70c	1.33432860539E-03
22049.70c	9.79193110454E-05
22050.70c	9.37599157158E-05
25055.70c	8.71513678950E-04
26054.70c	1.05952337437E-03
26056.70c	1.66322374761E-02
26057.70c	3.84109417430E-04
26058.70c	5.11182229355E-05
28058.70c	3.18268353245E-04
28060.70c	1.21673874326E-04
28061.70c	5.26856163138E-06
28062.70c	1.67366321839E-05
28064.70c	4.24408614207E-06

Table 4: TZM definition

Element	Atomic fraction
06000.71c	1.58717357426E-03
22046.71c	8.21398817036E-04
22047.71c	7.40752397576E-04
22048.71c	7.33982059287E-03
22049.71c	5.38638489983E-04
22050.71c	5.15738824497E-04
40090.71c	4.30062906719E-04
40091.71c	9.37863078587E-05
40092.71c	1.43354293911E-04
40094.71c	1.45276838425E-04
40096.71c	2.34047827781E-05
42092.71c	1.46562897947E-01
42094.71c	9.13549059328E-02
42095.71c	1.57229196575E-01
42096.71c	1.64735113705E-01
42097.71c	9.43177663103E-02
42098.71c	2.38312849463E-01
42100.71c	9.51078622417E-02

Table 5: Mild Steel definition

The composition of mild steel, the density is 7. 7 g/cm^3

MCNP input	Isotope	Relative atomic fraction
6012.70c	^{12}C	0.00818805
6013.70c	^{13}C	8.856E-05
25055.70c	^{55}Mn	0.00402112
26054.70c	^{54}Fe	0.05718942
26056.70c	^{56}Fe	0.89775277
26057.70c	^{57}Fe	0.02073301
26058.70c	^{58}Fe	0.00275918
15031.70c	^{31}P	0.00071322
16032.70c	^{32}S	0.00065402
16033.70c	^{33}S	5.236E-06
16034.70c	^{34}S	2.9556E-05
16036.70c	^{36}S	1.3779E-07
14028.70c	^{28}Si	0.00725451
14029.70c	^{29}Si	0.00036837
14030.70c	^{30}Si	0.00024283

10.2. Source Terms

Calculations were performed with these two proton beam source terms:

1. 1 W/m average homogeneous beam loss across the DTL, as input for shielding design calculations [25, 26].

The source term for the 1W/m beam loss was developed in consistency with the model used for the ESS accelerator prompt radiation shielding design assessment [1].

2. Four DTL tanks were modelled with beam on FC2, with no shielding, between DTL2 and DTL3 at 40 MeV and with a beam on FC4, with shielding, placed after DTL4 with an energy of 40 MeV and 74 MeV. Additionally, the impact of a higher beam energy of 76 MeV on the dose rate behind the TSW was calculated.

11. CALCULATIONS

11.1. Beam on FC

In this section, results are presented for the beam on FC2 and FC4 calculations. The calculated neutron dose rates, which is the dominant component, behind the TSW are shown in Figs. 9 and 10, where the leakage through the ventilation chicane can be clearly seen. Fig. 11 shows the total dose rate up to the position of the fence placed 1.68 m behind the TSW. The position of the second fence is determined as described in section 13. A summary of the results behind the wall and the position of the fence for the three cases is given in Table 5.

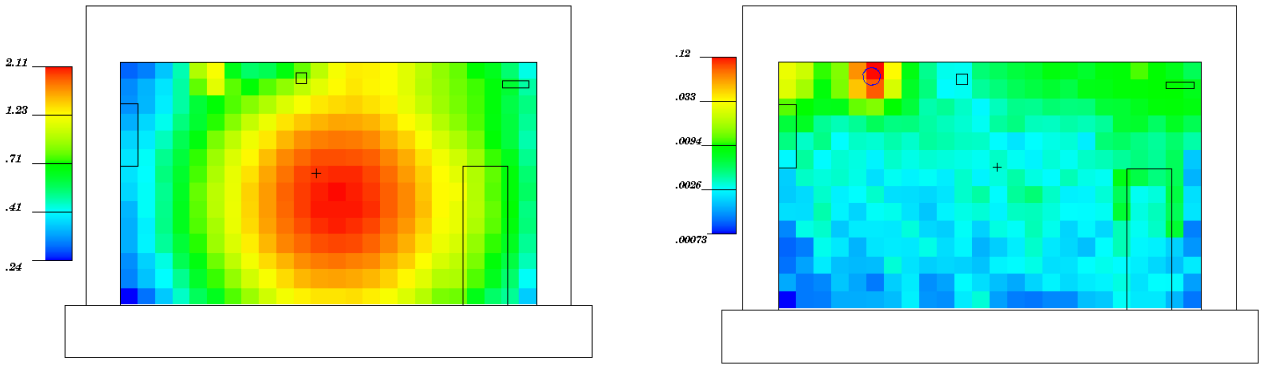

Figure 9: Neutron dose-rate profiles on the surface of the TSW for 74 MeV (left) and 40 MeV (right) on FC4. Units are in µSv/(µA hr).

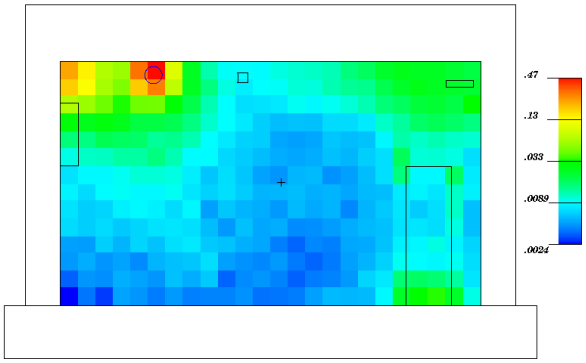

Figure 10: Neutron dose-rate profile on the surface of the TSW for 40 MeV on FC2. Units are in µSv/(µA hr).

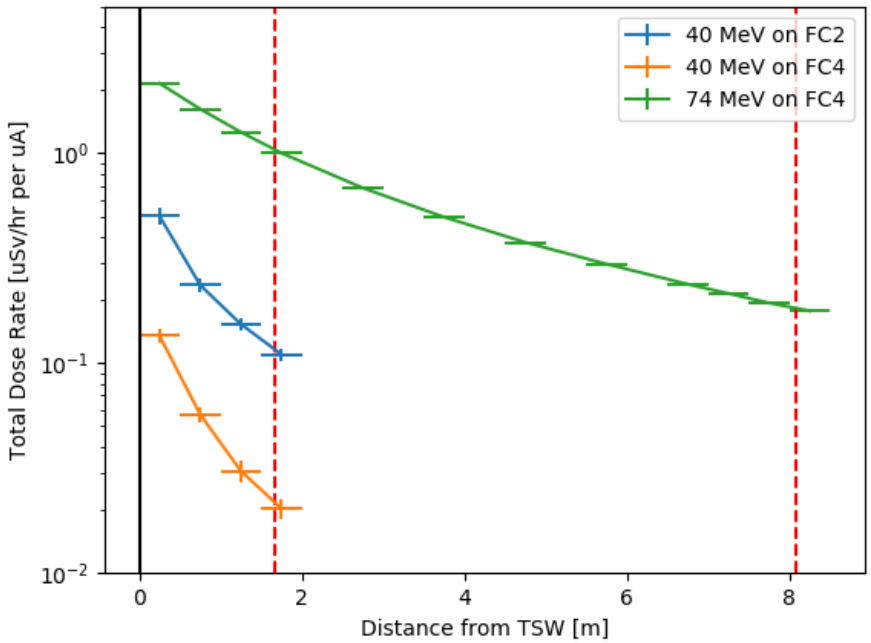

Figure 11: Maximal dose rates behind the TSW . The solid black line marks the surface of the TSW and the red-dashed lines are the positions of the fences. The position of the second one is determined as described in section 13.

Table 5: Maximal combined neutron and photon dose rates for the cases in Figures 9-11 at the indicated positions. Units in µSv/(µA hr) for beam on FC.

Case	TSW surface	Fence position	8.07 meters
4DTLs and FC2 at 40 MeV	0.50±0.05	0.11±0.01	-
4DTLs and FC4 at 40 MeV	0.13±0.01	0.020±0.002	-
4DTLS and FC4 at 74 MeV	2.15±0.01	1.00±0.01	0.183±0.001

Additionally, Table 5 also shows the dose rate at the 8.07 m position for 74 MeV on FC4. This location defines where a second fence could be installed.

11.2. 1 W/m source term

Results are presented for the 1 W/m source term in this section. The left panel of Fig. 12 shows the total dose rate on the surface of the TSW and the right panel shows the dose rate as a function of distance from the TSW to to the fence placed 1.68 m downstream. The dose rate is extrapolated out to 8.07 m using a 1/r function. Table 6 gives a summary of the results at the TSW surface, the position of the first fence and also at 8.07 m from the TSW surface

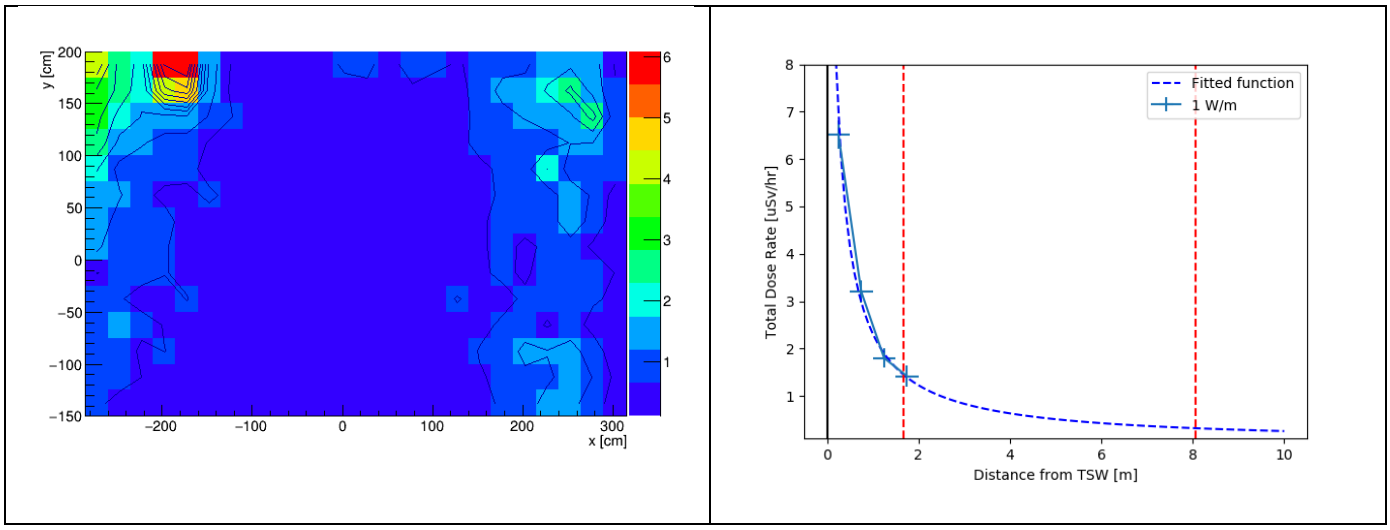

Figure 12: Maximal dose rate on the surface of the TSW (left) and as a function of distance from the TSW (right) for the 1 W/m source term. Units are in µSv/hr. The two red dashed lines indicate the positions of the fences. The position of the second one is determined as described in section 13.

Table 6: Maximal combined neutron and photon dose rates for the case in Figure 12 at the indicated positions for the 1 W/m source term. Units are in µSv/hr.

Case	TSW surface	Fence position	8.07 meters
1 W/m	6.52±0.29	1.42±0.23	0.32±0.02

11.3. Impact of higher beam energy

The impact of a higher beam energy of 76 MeV was also investigated. The calculations above were repeated by changing the primary energy for beam on FC to 76 MeV and also increasing the beam energy along the linac by 3% for the 1 W/m source term calculations. The results are reported in Table 7.

Table 7: Maximal combined neutron and photon dose rates for the impact of an increased beam energy to 76 MeV. Units are in µSv/hr.

Case	TSW surface	Fence position	8.07 meters
4DTLS and FC4 at 76 MeV	2.70±0.01	1.26±0.01	0.24±0.01
1 W/m for 76 MeV case	6.61±0.20	1.43±0.11	0.34±0.03

The results show an increase in the dose rates at the three selected positions for the beam on FC4 while the differences for the 1 W/m source term are not significant within the errors of the two sets of calculations.

12. TUNNEL AIR ACTIVATION

For the 74 MeV proton beam on the Faraday Cup, a list of produced isotopes and their production rates in the tunnel air were calculated. No ventilation was assumed and production rates were calculated for the section up to the end of DTL 4 (TSW location) per µA of incident beam current (Table 8).

Table 8: Unstable nuclide production rates in the normal conducting linac air for 74 MeV proton beam on the faraday cup per µA of incident beam current

Nuclide	Z	A	Production rate [1/(s µA)]	Statistical error [%]	Nuclide	Z	A	Production rate [1/(s µA)]	Statistical error [%]
H	**1**	**3**	105 000	0.003	Al	13	30	1.928	0.720
He	2	5	7.935	0.355	Al	13	31	0.454	1.485
He	2	6	311.800	0.057	Si	14	31	34.900	0.169
Li	3	8	1407	0.027	Si	14	32	8	0.354
Li	3	9	2.438	0.640	Si	14	33	1.077	0.964
Be	4	6	784.900	0.036	Si	14	34	1.474	0.824
Be	**4**	**7**	121 000	0.003	P	15	30	16.200	0.248
Be	4	8	0.567	1.328	P	15	32	123.200	0.090
Be	4	10	3057	0.018	P	15	33	391.400	0.051
Be	4	11	2640	0.019	P	15	34	157.500	0.080
B	5	8	2186	0.021	P	15	35	24.960	0.200
B	5	12	14 980	0.008	P	15	36	1.872	0.731
B	5	13	144.500	0.083	P	15	37	1.134	0.939
C	6	8	6.014	0.408	S	16	30	0.170	2.425
C	6	9	236.600	0.065	S	16	31	0.453	1.485
C	6	10	48 610	0.005	S	16	35	664.600	0.039
C	6	11	280 000	0.002	S	16	37	186	0.073
C	6	14	88 050	0.003	S	16	38	236.100	0.065
C	6	15	0.288	1.865	Cl	17	32	1.362	0.857
N	7	12	16 120	0.008	Cl	17	33	4.368	0.478
N	7	13	152 200	0.003	Cl	17	34	69.460	0.120
N	7	16	4.586	0.467	Cl	17	36	2021	0.022
O	8	12	217.900	0.068	Cl	17	38	2097	0.022
O	8	13	5433	0.014	Cl	17	39	2184	0.021
O	8	14	164 100	0.002	Cl	17	40	0.567	1.328
O	8	15	163 100	0.002	Ar	18	33	0.339	1.718
F	9	18	0.057	4.200	Ar	18	34	1.134	0.939
Ne	10	23	0.057	4.200	Ar	18	35	14.101	0.266
Na	11	24	0.170	2.425	Ar	18	37	1715	0.024
Mg	12	27	0.453	1.486	Ar	18	39	4967	0.014
Al	13	26	0.057	4.200	**Ar**	**18**	**41**	170.400	0.077
Al	13	28	1.645	0.780	K	19	36	0.567	1.328
Al	13	29	1.132	0.940	K	19	37	5.107	0.443
					K	19	38	169.800	0.077

13. CONCLUSIONS AND RECOMMENDATIONS

Prompt dose rate for a beam on the Faraday cup The prompt dose rate was calculated for three different DTL configurations and the maximum dose rate results are shown in table 9 with the factor of two included.

Table 9: Maximal dose rates from Table 5 with the safety factor included. Units are in µSv/(µA hr).

Case	TSW surface	Fence position	8.07 meters
4DTLs and FC2 at 40 MeV	1.00±0.09	0.22±0.02	-
4DTLs and FC4 at 40 MeV	0.27±0.02	0.041±0.004	-
4DTLS and FC4 at 74 MeV	4.30±0.02	2.00±0.02	0.366±0.002

Prompt dose rate for 1 W/m Table 10 shows the results for the 1 W/m source term including the safety factor of 2 for the Monte-Carlo calculated values and a safety factor of 3 for the extrapolated value at 8.07 m. The contribution from the 1 W/m source term is to be scaled according to the procedure described in [6], and the values are given in the second row of Table 10.

Table 10: Maximal combined neutron and photon dose rates for the 1 W/m source term from Table 6 with safety factor included. Units in µSv/hr. The second row is scaled by the factor of 0.14, which is the worse case scaling according to [6].

Case	TSW surface	Fence position	8.07 meters
1 W/m	13.0±0.6	2.84±0.46	0.96±0.05
1 W/m Scaled	1.8±0.1	0.40±0.06	0.134±0.007

Position of the 2nd fence: The position of the second fence is determined by adding the scaled 8.07 meter position values from Table 9 and 10 together, which assumes the accelerator is operating at 1 µA. The scaling factor for the 1 W/m losses is 0.14 for the worse case operating scenario described in [6]. This results in 0.134 µSv/hr + 0.366 µSv/hr = 0.5 µSv/hr, which satisfies the requirements for a non-designated area.

Effect of the beam energy increased to 76 MeV: The effect of the beam energy increasing to 76 MeV can be calculated based on the procedure in the previous paragraph. Table 11 summarises the results with safety factors included. This gives a dose rate increase at the position of the second fence to be 0.62 µSv/hr, with safety factors included.

Table 11: Maximal combined neutron and photon dose rates for an increased beam energy to 76 MeV at the indicated positions. Units in µSv/hr. The second row is scaled by the factor of 0.14, which is the worse case scaling according to [6].

Case	TSW surface	Fence position	8.07 meters
4DTLS and FC4 at 76 MeV	5.40±0.02	2.52±0.02	0.48±0.02
1 W/m for 76 MeV scaled	1.85±0.06	0.40±0.03	0.14±0.01

Air activation Nuclide production rates in the normal conducting linac for 74 MeV are listed (without a safety factor) in Table 7, per µA of incident beam.

14. REFERENCES

[1] N. Mokhov, I. Tropin, I. Rakhno, Y.I. Eidelman, and L. Tchelidze. ESS accelerator prompt radiation shielding design assessment. ESS-0052477, April 2016.

[2] Lena Johansson. ESS Handbook for Radiation Protection Chapter 2. General Radiation Protection Rules. ESS-0239718, Revision 5.

[3] B. Cheymol. Faraday cup design specifications for the ESS DTL. ESS-0043439, November 2017.

[4] Mamad Eshraqi. Normal conducting linac beam commissioning scenarios and steps. ESS-0149990, December 2017.

[5] Sigrid Kozielski, ESS procedure for designing shielding for safety. ESS-0019931, Feb 2019.

[6] Mamad Eshraqi, Scaling of the current, losses and doses during commissioning, ESS-1563794, Oct. 2019.

[7] C. J., MCNP Users Manual – Code Version 6.2 LA-UR-17-29981 (2017)

[8] K.K. Gudima, S.G. Mashnik, and V.D. Toneev. Cascade-exciton model of nuclear reactions. Nuclear Physics A, 401(2):329-361, 1983.

[9] S.G. Mashnik, K.K. Gudima, R.E. Prael, A.J. Sierk, M.I. Baznat, and N.V. Mokhov. CEM03.3 and LAQGSM03.03 event generators for the MCNP6, MCNPX, and MARS15 transport codes. Invited lectures presented at the Joint ICTP-IAEA Advanced Workshop on Model Codes for Spallation Reactions, LANL Report LA-UR-08-2931, Los Alamos, arXiv:0805.0751, February 2008.

[10] S.G. Mashnik and A.J. Sierk. CEM03.03 User Manual. LANL Report, LA-UR-12-01364, Los Alamos, 2012.

[11] M.B. Chadwick, P. Oblozinsk_y, M. Herman, N.M. Greene, R.D. McKnight, D.L. Smith, P.G. Young, R.E. MacFarlane, G.M. Hale, S.C. Frankle, A.C. Kahler, T. Kawano, R.C. Little, D.G. Madland, P. Moller, R.D. Mosteller, P.R. Page, P. Talou, H. Trellue, M.C. White, W.B. Wilson, R. Arcilla, C.L. Dunford, S.F. Mughabghab, B. Pritychenko, D. Rochman, A.A. Sonzogni, C.R. Lubitz, T.H. Trumbull, J.P. Weinman, D.A. Brown, D.E. Cullen, D.P. Heinrichs, D.P. McNabb, H. Derrien, M.E. Dunn, N.M. Larson, L.C. Leal, A.D. Carlson, R.C. Block, J.B. Briggs, E.T.

Cheng, H.C. Huria, M.L. Zerkle, K.S. Kozier, A. Courcelle, V. Pronyaev, and S.C. van der Marck. ENDF/B-VII.0. Nucl. Data Sheets, 102:2931, 2006.

[12] A.J. Koning and D. Rochman, Nucl. Data Sheets, 113 (2012) 2841

[13] Koji Niita, Norihiro Matsuda, Yosuke Iwamoto, Hiroshi Iwase, Tatsuhiko Sato, Hiroshi Nakashima, Yukio Sakamoto, and Lembit Sihver. PHITS: Particle and Heavy Ion Transport code System, Version 2.23. JAEA-Data/Code 2010-022, 4 Oct 2010.

[14] A. Boudard, J. Cugnon, J.-C. David, S. Leray, and D. Mancusi. New potentialities of the Liège intranuclear cascade model for reactions induced by nucleons and light charged particles. Phys. Rev., C(87):014606, 2013.

[15] S. Furihata. Statistical analysis of light fragment production from medium energy protoninduced reactions. Nucl. Instrum. Meth., B(171):251-258, 2000.

[16] T. Sato et al., Features of Particle and Heavy Ion Transport System (PHITS) version 3.02, J. Nucl. Sci. Technol. 55, 684-690 (2018).: PHITS ver. 3.10 User's Manual

[17] M.B. Chadwick et al., Nuclear Data Sheets, 112, 2887-2996 (2011);

[18] D. A. Brown et al., Nuclear Data Sheets 148,1-142 (2018)

[19] A. Boudard et al., Phys. Rev C87, 014606 (2013)

[20] K. Iida, A. Kohama, and K. Oyamatsu, J. Phys. Soc. Japan 76, 044201 (2007)

[21] Stuart Ansell. CombLayer: A fast parametric MCNP(X) model constructor. In ICANS XXI, pages 148-154, Mito, Japan, September 2014. DOI:10.11484/jaea-conf-2015-002, JAEA, https://github.com/SAnsell/CombLayer.

[22] S.W. Mosher et al., ADVANTG—An Automated Variance Reduction Parameter Generator, ORNL/TM 2013/416 Rev. 1, Oak Ridge National Laboratory (2015).

[23] ESS-0416081, Neutronic design of the bunker wall and roof

[24] L. Zanini, A. Takibayev, and F. Mezei. Materials definition to be used in Monte Carlo calculations. EDMS-1188675, January 2012. ESS Design Update WP3.

[25] Renato De Prisco, Mamad Eshraqi, and Anders Karlsson. Effect of the field maps on the beam dynamic of the ESS drift tube linac. In IPAC2015, Richmond, VA, USA, 2015.

[26] Lali Tchelidze. Input criteria for shielding calculations and hands on maintenance conditions for ESS accelerator. ESS-0008351, March 2018.

DOCUMENT REVISION HISTORY

Revision	Reason for and description of change	Author	Date
1	First issue	Konstantin Batkov Lali Tchelidze	2017-10-20
2	Second issue (the document version in first issue was wrong, this was corrected)	Konstantin Batkov Lali Tchelidze	2017-10-25

Revision	Reason for and description of change	Author	Date
3	SkanskaConcrete definition correct; TSW geometry changed from 3 to 1 wall; statistical errors added for the tunnel air activation results	Konstantin Batkov	2018-09-26
4	An internal review has caught some inconsistencies and shortcomings in the previous version of this document. The current document is an update, and the issues presented in the open items section are still not resolved, but are being worked on Report is transferred to docx format	Douglas Di Julio Konstantin Batkov	2019-07-04
5	Addressed open issues in last revision, added DTL results from different DTL configurations, and added the chicane in the TSW. Activation results are kept from a previous draft.	Douglas Di Julio	2019-10-02
6	Added reference to ESS-1563794 for the scaling of beam losses	Douglas Di Julio	2019-10-30
7	Removal of obsolete reference and minor revisions	Douglas Di Julio	2019-11-26
8	Addition of data for the position of a second fence when running at 74 MeV	Douglas Di Julio	2020-01-21
9	Addition of results for 76 MeV Minor updates throughout	Douglas Di Julio	2020-08-14
10	Corrected typos in Section 13	Douglas Di Julio	2020-08-17